

## Palaeomagnetic cave stratigraphy of sediments from Hellemofjord, northern Norway

Reidar Løvlie,<sup>1</sup> Kari Lise Ellingsen<sup>1</sup> and Stein-Erik Lauritzen<sup>2</sup>

<sup>1</sup>*Institute of Solid Earth Physics, Allégt. 41, N-5007 Bergen, Norway*

<sup>2</sup>*Department of Geology, Allégt. 41, N-5007 Bergen, Norway*

Accepted 1994 August 19. Received 1994 June 20; in original form 1993 August 19

### SUMMARY

Subglacial deposited sediments from three deep karst caves in Nordland, northern Norway, carry single-component palaeomagnetic directions interpreted to represent discrete records of palaeosecular variations (PSV) defining a clockwise rotation of the vector with time. The results suggest that preserved sediment sections commenced accumulating at the highest altitude in this cave system, consistent with an inverse stratigraphic sedimentation. Anomalously low inclinations are interpreted to represent a detrital remanent magnetization acquired at the time of deposition and affected by inclination error. The preservation of the inclination error in these sterile sediments is attributed to the absence of processes that may cause post-depositional alignment of magnetic grains. Non-systematic directional scatter is also attributed to poor smoothing of geomagnetic field variations in these cave sediments compared with lacustrine deposits. The almost closed PSV loop may represent discrete periods of sedimentation during one or, alternatively, several subglacial events. The PSV loop exhibits amplitudes in declination and inclination comparable with Holocene or Weichselian lacustrine PSV records. The minimum duration of sediment accumulation may be of the order of 400 to 1000 yr. If the investigated sediments represent succeeding records of geomagnetic secular variations during the last Late Weichselian glacial retreat, the reasonably good correlation with the PSV records from the Torreberga (Southern Sweden) varved clay sequence (12 200–10 200 BP) and UK lacustrine sediments (0–10 000 BP) tentatively suggests that the Rågge Javre Raigi sediments accumulated during the final Weichselian glacial retreat between 10 900 and 9 800 BP.

**Key words:** cave sediments, chronostratigraphy, DRM, Late Weichselian, palaeomagnetism.

### INTRODUCTION

Sediments in karst caves in northern latitudes are often devoid of biological material and speleothem strata. The sedimentary sequences are therefore difficult to date with radiometric methods. Karst caves in formerly glaciated terrains often contain deposits, the surface counterparts of which have in general been removed by glacial erosion. In order to establish a chronostratigraphy within or between cave systems of this type, one must hence rely on lithostratigraphic criteria or applying palaeomagnetic stratigraphy. However, even if palaeomagnetic polarity patterns are encountered in cave sediments, as has been reported from fine-grained sediments in different cave systems (Creer & Kopper 1974, 1976; Noel 1987), this may only indicate sediment ages greater than the Brunhes/Matuyama

boundary (0.78 Ma) (Cande & Kent 1992) since sedimentation rates in caves are in general unknown and reliable age assessment is precluded by the inherent inability of palaeomagnetic polarity patterns to provide unique chronologies. Also, geomagnetic reversals are rare events on a Quaternary time-scale, restricting the application of reversal stratigraphy to sediments with slow accumulation rates. Palaeomagnetic secular variation records retained in Holocene lacustrine sediments appear to have potential time resolutions of some hundreds of years (Thompson 1983), which is within the expected time frame for sediment accumulation in subglacially exposed cave systems. Dating of fine-grained cave sediments by correlating palaeosecular variation records has previously been reported from the Grønligrotta and Jordbruksgrotta caves in northern Norway (Noel & St. Pierre 1984). Patterns of declination and

inclination were correlated with the Holocene PSV record from Lac du Joux lacustrine sediments yielding an age-span for sediment deposition at these sites between 9800 and 6000 yr BP. This suggested time-span, however, partially post-dates nearby end moraines which provide minimum ages for the glacial cover required for sediment accumulation to take place. This latter argument was forwarded by Løvlie *et al.* (1988) who proposed a more realistic time-span for sediment deposition of these sites between 9200 and 9800 yr BP by correlation with the UK PSV master curve (Thompson & Turner 1979).

At the present state of palaeomagnetic research, PSV records with acceptable precision are only encountered in relatively rapidly deposited sediments (several mm yr<sup>-1</sup>). In phreatic cave systems, rapidly deposited sediments may have accumulated under the influence of unidirectional water flow along the axis of conduits.

The present study reports on palaeomagnetic investigations of sediment sequences sampled from three deep karst

caves in Nordland, northern Norway, with the objectives of elucidating within-cave stratigraphies and constructing chronostratigraphic time frames based on PSV records in order to explore the relationship between accumulative and erosive processes during glacial advances and retreats.

## GEOLOGY AND SAMPLING

Hellemofjord represents the southern part of the Tysfjord fjord–valley complex in Nordland, consisting of crystalline basement windows surrounded by metasediments (Fig. 1). Hellemofjord cuts through a synclinal structure outcropping as subvertical strata of mica schist, gneiss and marbles. The almost vertical carbonate sheets and large-scale east–west fracturing provide excellent conditions for deep karstification (Lauritzen, Kyselak & Løvlie 1991). The three investigated caves are situated within carbonate bands with maximum thicknesses less than 30 m (Fig. 2).

Remnant sediment sequences of varying thicknesses are

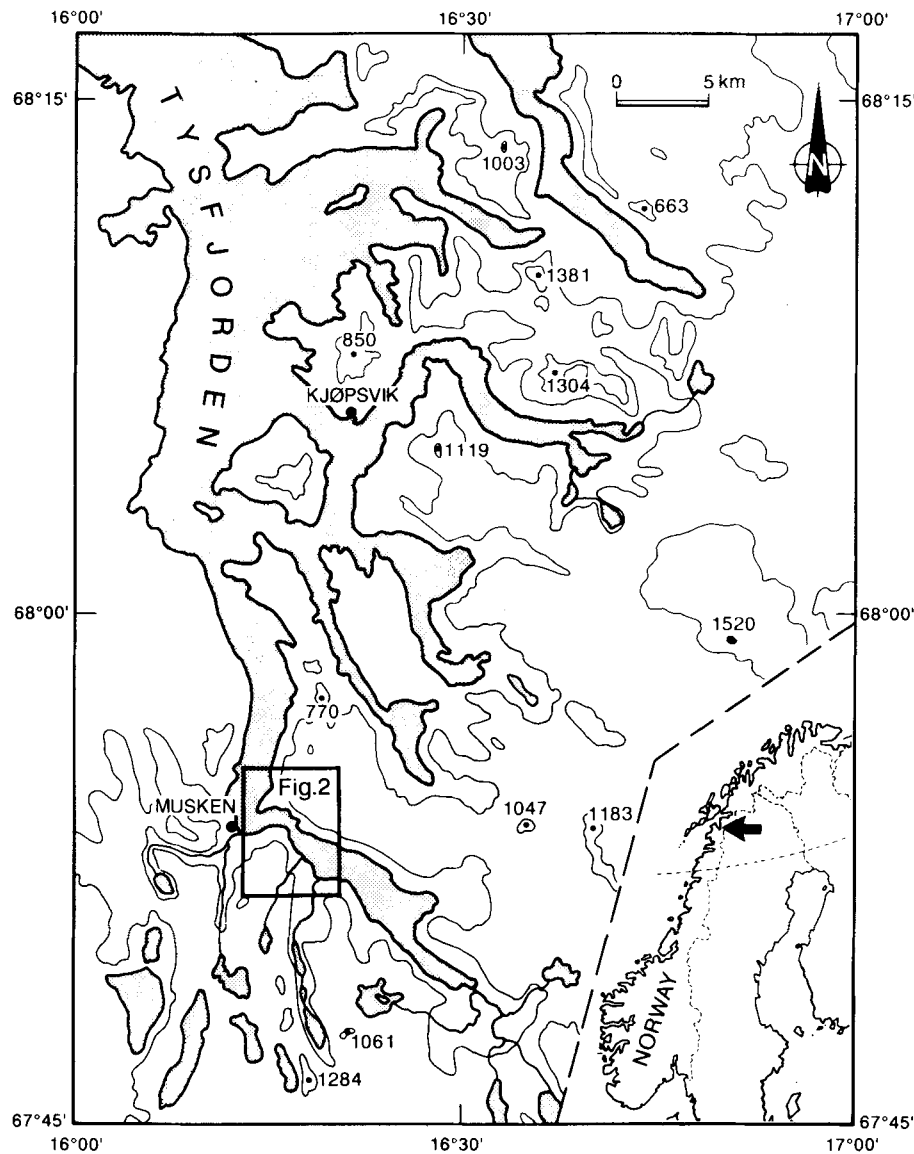


**Figure 1.** Sketch map of the Tysfjord fjord–valley complex. Dark shade: fjords and lakes. The paleic plateaus are depicted by contours at 500, 1000 and 1500 m above sea-level.

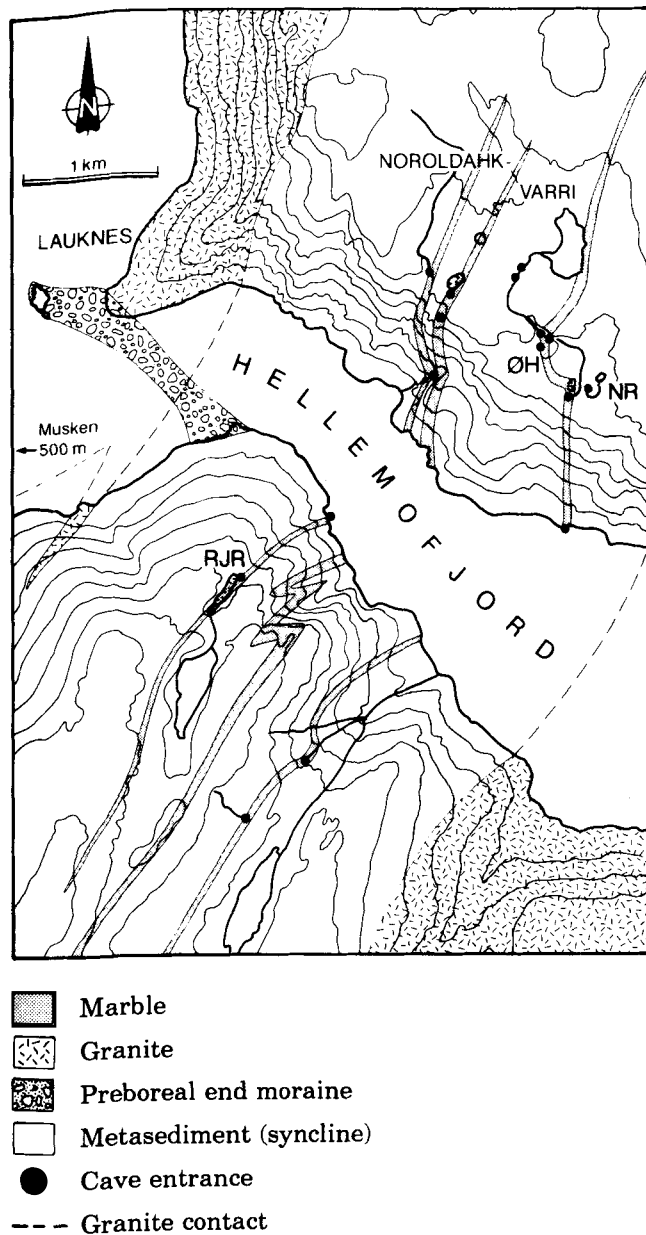


**Figure 2.** Topographic map of the Hellemofjord stripe karst. RJR, Rågge Javre Raigi cave; ØH, Østhullet cave; NR, Noroldakh-Raigi cave. Contour intervals 100 m. A Preboreal end-moraine is exposed at the Lauknes peninsula.

preserved in small, isolated deposits. The sediments vary from silt-sand through silty clay to almost pure clay. The small thickness of the sediment sections, absence of biological activity, almost constant temperatures (>0 °C), as well as high humidities, have preserved the sediments with an unusually low degree of consolidation and cementation. Coarser sediments (sand) were generally so poorly consolidated that sampling of the sparse sections was not possible. The age(s) of the sediment sequences are not known. They are all situated above the local maximum sea-level for the Late Weichselian and must therefore have accumulated subglacially during Late Weichselian or older glacial advances or retreats (youngest retreat c. 10 000 BP).

Oriented samples were collected either by pushing

cylindrical sample boxes (20 × 21 mm diameter) into the cleaned sediment surface (Løvlie 1989a), or by carving out 'bars' of sediments that were placed in aluminium U-channels (2.5 × 3 × 50 cm) which were subsequently subsampled in the laboratory. The latter procedure is regarded as the most reliable and time-effective, but is not applicable to the thin layers of sediment present in the Noroldakh-Raigi and Østhullet caves.

The stratigraphic positions of the sampling locations are shown in Fig. 3.

### Rågge Javre Raige (RJR)

Four sediment sections were sampled within this cave system.

#### Site 1

Site 1 (560 m a.s.l.) is a small rectangular (1.5 × 2.5 m) deposit discovered accidentally by digging into the sediment surface in a small inconspicuous alcove situated c. 1 m above the general path, some 150 m from the upper entrance. The c. 90 cm section of partly laminated silt and clay sediments filling a small 'basin' between boulders originating from the roof was capped with a 1 cm thin layer of unbroken caliche, implying the absence of surficial deformation probably since the last subglacial period. The section has been divided into eight lithological units (A–H, Fig. 4) based on changes in colour of the sediment. Some of the inferred lithological boundaries are associated with abrupt changes in palaeomagnetic properties (Fig. 4) attributed to discontinuous sedimentation or erosive events of unknown duration and magnitude. The central, most extensive part of the 'basin' was sampled with two U-channels, while the eastern limb was completely confined within a single U-channel (Fig. 5).

#### Site 2

Site 2 (554 m a.s.l.), situated some 30 m away from Site 1, probably represents a lateral wedging out along the cave passage of some layers retained in the former deposit. Three small pits (0.5 × 0.5 m) were dug at 5–8 m intervals into the 30–40 cm thick sediment cover. The sections consisted of a coarse-grained (pebbles, clasts) unit (3–7 cm thick) resting on bedrock, succeeded by a homogeneous silt unit interbedded with one or two 4–8 cm thick, finely laminated silty clay layers. The top 8–15 cm of the sequence consists of loose silt. This unit was not sampled due to the low degree of consolidation and the fact that cavers certainly must have deformed the silt layer by walking. Five to seven oriented samples were collected from the 4–8 cm thick laminated silty clay layer only. Samples of clay-silt sediments were also collected from the 'Clay Pot' (Lauritzen *et al.* 1991) (490 m a.s.l.) which is the landing spot for cavers after descending a c. 20 m vertical section of the 'Main Slide'. Although deformational features were not evident within the c. 50 cm thick partly homogeneous sediment cover, anticipated anomalous palaeomagnetic directions were

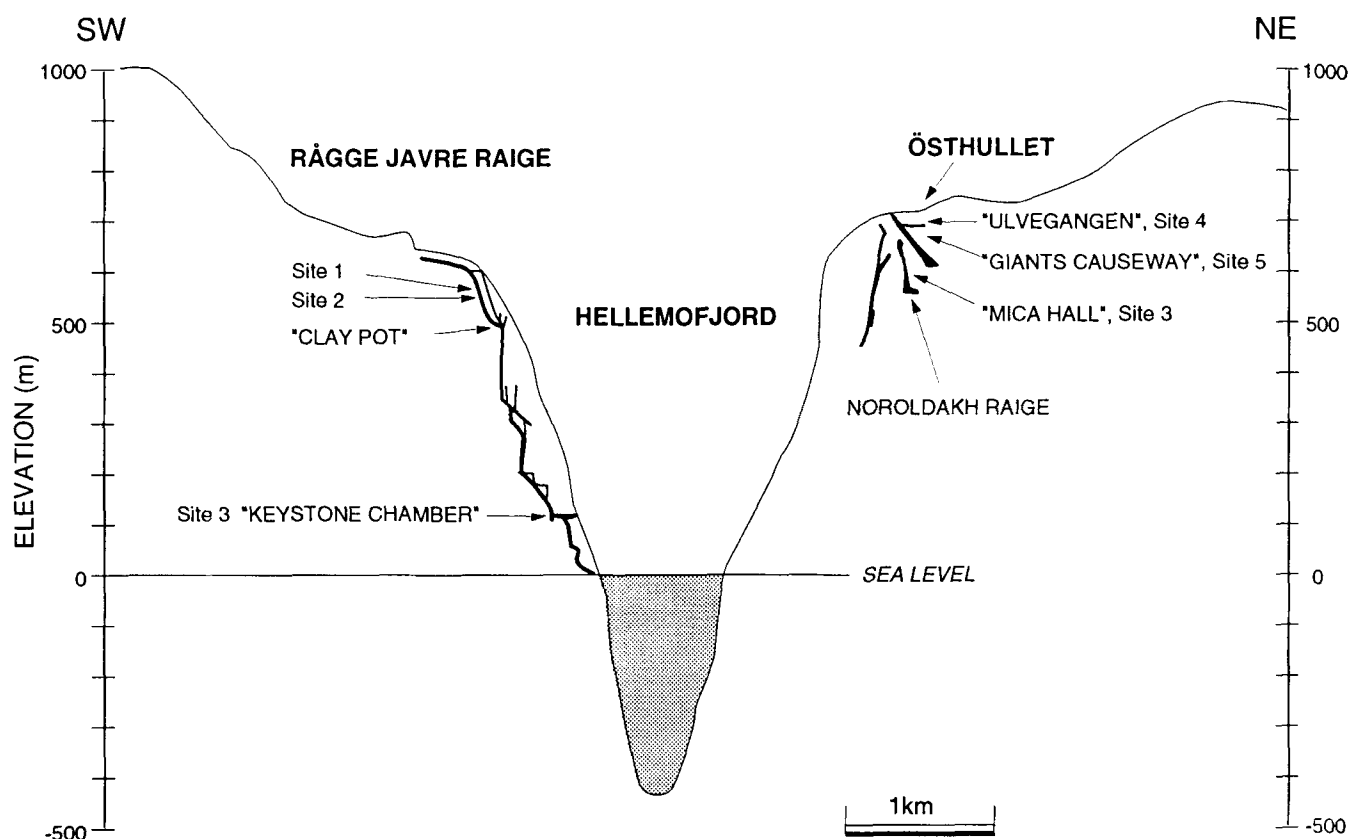


**Figure 3.** Stratigraphic sampling locations in the Rågge Javre Raigi, Østhullet and Noroldakh-Raigi cave systems shown on a vertical NW-SE section of the stripe karst across the Hellemofjord.

indeed encountered (Fig. 6). These results are hence omitted from further analysis. This observation puts some serious constraints on the application of palaeomagnetic stratigraphy of sediment sections in caves exposed to extensive human activity.

#### Site 3

Site 3 (above the 'Keystone chamber') (120 m a.s.l.) represents a *c.* 1 m thick partly laminated clay-silt section, situated in the corner of a passage not likely to have been exposed to heavy shocks by cavers. The sediment apparently wedges out towards the walls of the cave. This section has been divided into five units (a-e, Fig. 7) based on colour variations. Abrupt variations in palaeomagnetic properties across some of the inferred lithological boundaries (Fig. 7) are attributed to discontinuous sedimentation or erosive events of unknown duration and magnitude. The thickest section was sampled by two partly overlapping 60 cm long U-channels, while the thinner section, by the wall, was sampled by a single U-channel. A pronounced light-coloured silt unit, some 3 cm thick, provides a unique stratigraphic correlation between the sampled sediments.

#### Østhullet (ØH)

Sections (*c.* 0.5 m) of undeformed sediments consisting of horizontal units of clay, silt and sandy clay were encountered between large boulders at two levels in this cave. At Site 4, 'Ulvegangen' (705 m a.s.l.), five oriented

samples were collected from the lowermost layer of homogeneous sandy clay. From an almost identical section at Site 5, 'Giants Causeway' (670 m a.s.l.), seven oriented samples were obtained.

#### Noroldakh-Raige (NR)

Site 6 is a small 0.5 m section consisting of sand clasts interbedded with silt lamina situated between large boulders in the 'Mica Hall' (600 m a.s.l.), from which seven samples were collected.

### PALAEOMAGNETIC AND ROCK-MAGNETIC PROCEDURES

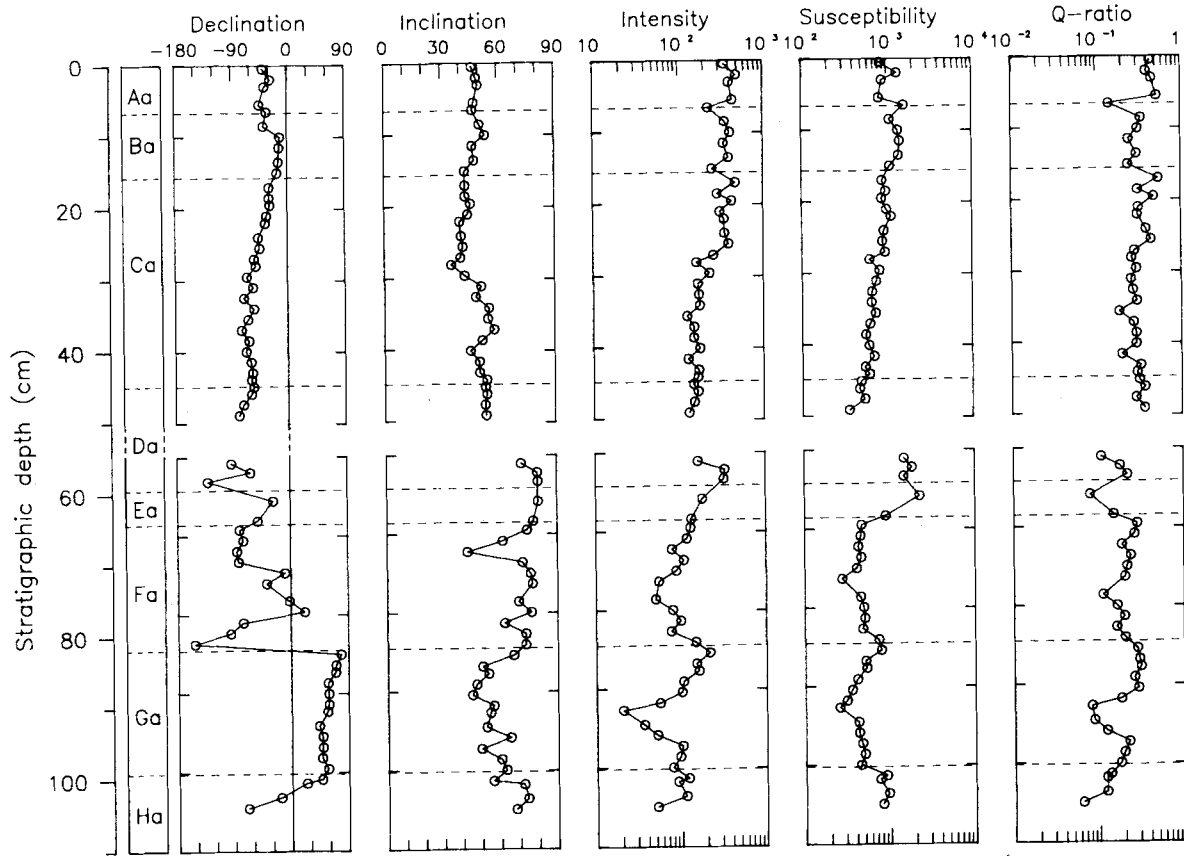
The direction and intensity of the natural remanent magnetization (NRM) were determined on either a Digico spinner magnetometer or a three-axis SQUID magnetometer (Cryogenic Consultants Ltd). All samples were subjected to progressive alternating field (a.f.) demagnetization in 5–10 mT steps to a maximum of 60–70 mT in a two-axis tumbler. The anisotropy of magnetic susceptibility (AMS) was determined on all samples using a KLY-2 induction bridge (sensitivity:  $4 \times 10^{-9}$  SI).

Progressive acquisition of isothermal remanent magnetization (IRM) on several samples from each section was achieved using a solenoid up to 0.24 T and a 4" Newport electromagnet to 0.97 T.

Thermomagnetic analysis on dried 20–50 mg samples of sediment was performed in a transverse Curie balance by

Site 1

(a) Reference section



(b) East section of small 'basin'

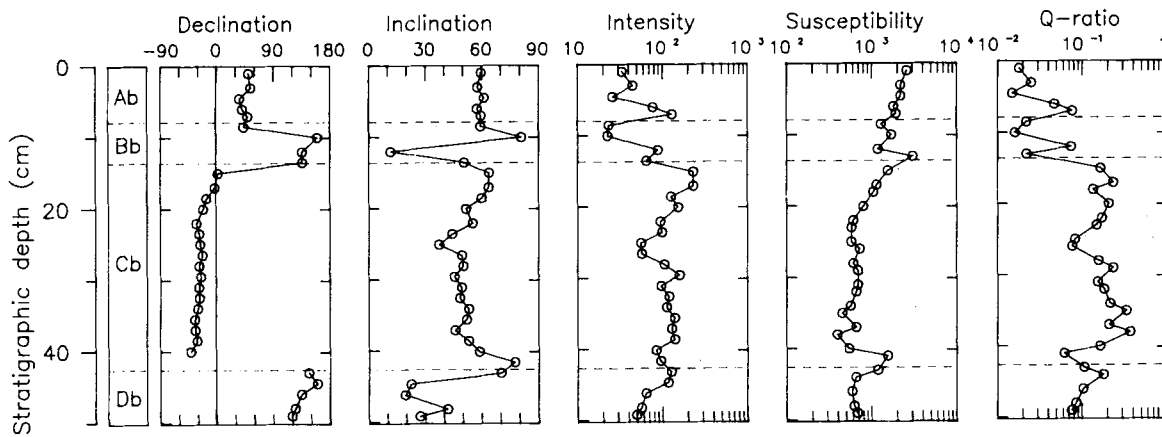


**Figure 4.** Rågge Javre Raigi cave Site 1: stratigraphic variations of ChRM declination, inclination, NRM intensity ( $\text{mA m}^{-1}$ ), susceptibility ( $\kappa$ ,  $10^{-6} \text{SI}$ ) and  $Q$ -ratio ( $\text{NRM}/\kappa$ ). (a) Reference section from central part of 'basin'. (b) East section of small 'basin'. Major lithostratigraphic boundaries indicated by broken horizontal lines. Simplified lithostratigraphy shown in left column: A, silt-clay; B, channel sand; C, laminated silt, D, clay; E, fine sand; F, inclined laminated silt; G, tectonized silty clay; H, sandy silt with clay clasts.

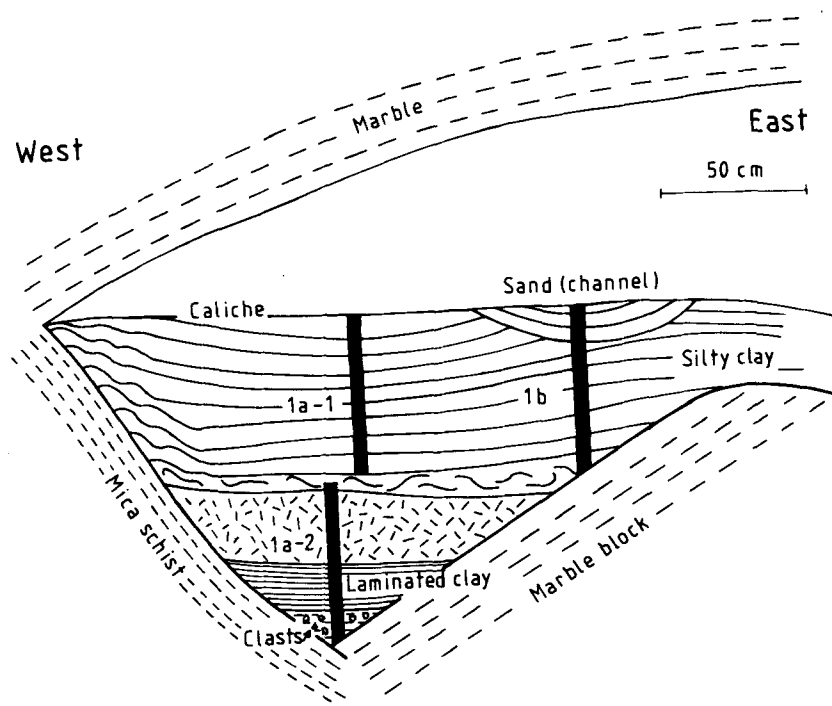


**Figure 5.** Simplified lithostratigraphic sketch of the Site 1 sequence. Sampling positions of U-channels and major lithological units are indicated. (a) reference section collected from the central part of the small 'basin' consisting of eight lithological units: reference section Fig. 4a. (b) Section from the eastern section of the 'basin' consisting of four lithological units (Fig. 4b).

## Clay Pot

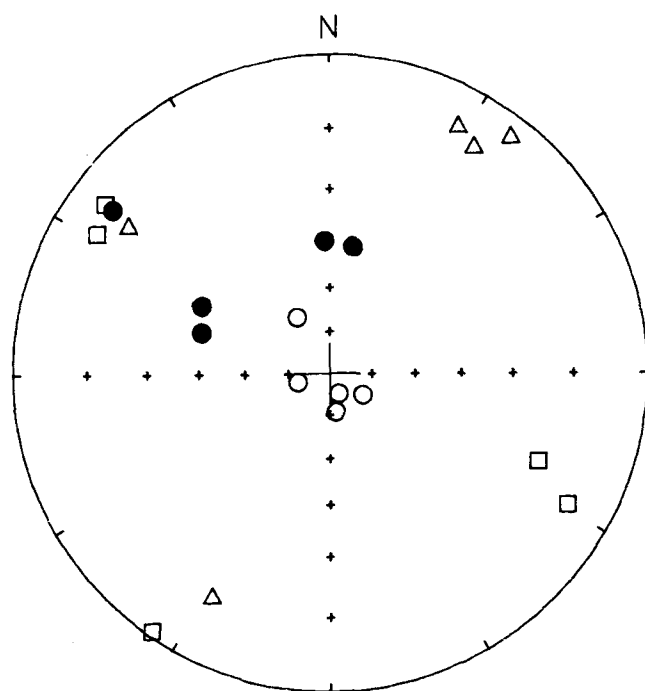


**Figure 6.** The 'Clay Pot' site: stereographic projection showing directions of the characteristic remanent magnetization (small circles) and of the principal susceptibility axes ( $k_1$ , square;  $k_2$ , triangle;  $k_3$ , circle; all lower hemisphere). Prolate susceptibility ellipsoids are interpreted to reflect a partially deformed magnetic fabric, and this site has been omitted from further analysis since the inferred deformation is likely also to have affected the palaeomagnetic directions.

heating in air ( $20^\circ \text{min}^{-1}$ ) to a maximum temperature of  $700^\circ\text{C}$  in a field of 0.45 T. In addition, magnetic hysteresis curves were obtained on three samples on a MiniMag vibrating sample magnetometer (VSM) at the Gif sur Yvette palaeomagnetic laboratory.

## MAGNETIC CONSTITUENTS

### IRM analysis

IRM acquisition curves saturate in fields less than 300 mT (Fig. 8a). The remanent acquisition coercive force (RACF) ranges between 60 and 110 mT and the remanent coercive forces (RCF) between 40 and 80 mT. Samples with the highest RACF often show curves with the characteristic initial linear plateau indicative of single-domain particles (Cisowski 1981). Saturation close to 300 mT, high values of RCF and RACF are diagnostic of fine-grained magnetite/maghemite, also evidenced by the values of the ratio RACF/RCF (1.3–1.65) which lie within the empirically derived range for pure magnetite (Dankers 1981) (Fig. 8b).

### Thermomagnetic analysis

The high field magnetization versus temperature heating curves define a single Curie temperature ( $T_c$ ) in the  $570$ – $580^\circ\text{C}$  range, diagnostic of pure magnetite ( $T_c = 580^\circ\text{C}$ ) (Fig. 8c). The high field-induced magnetization at  $700^\circ\text{C}$  varies between 5 and 30 per cent of the initial value, indicating significant contributions from paramagnetic mineral phases. The magnetite  $T_c$  also appears on most of the cooling curves, but in a few cases it is absent, probably due to oxidation of fine-grained magnetite to haematite or, alternatively, to the inversion of maghemite to haematite (Fig. 8d).

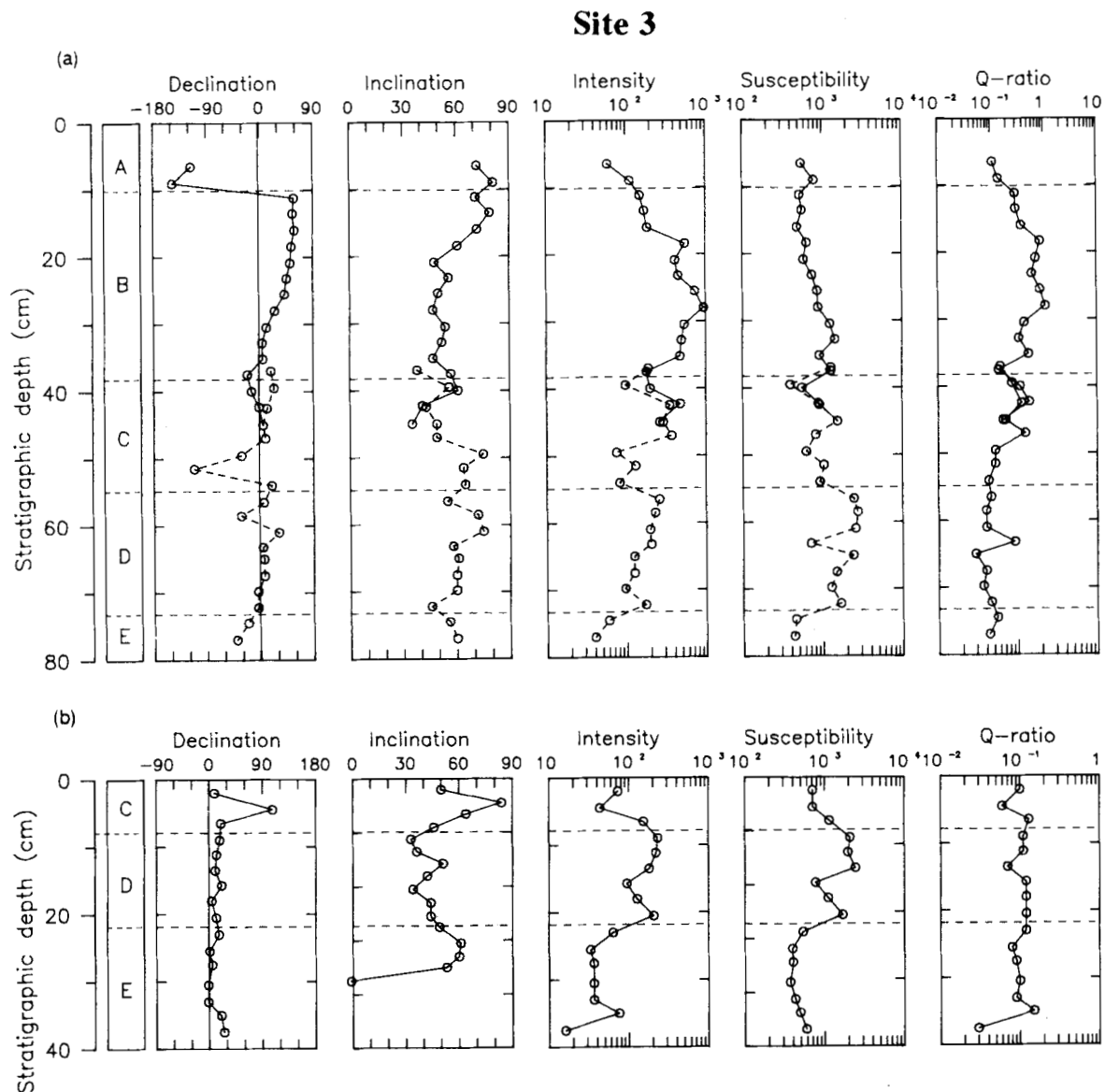


**Figure 7.** Rågge Javre Raigi Site 3: stratigraphic variations of ChRM declination, inclination, NRM intensity ( $\text{mAm}^{-1}$ ), susceptibility ( $\kappa$ ,  $10^{-6}$  SI) and  $Q$ -ratio ( $\text{NRM}/\kappa$ ). (a) Central sequence. (b) Shortest section close to the wall of the passage. Major lithostratigraphic boundaries indicated by broken horizontal lines. Simplified lithostratigraphy to the left: A, silt-clay; B, channel sand; C, laminated silt; D, clay; E, fine sand.

### Hysteresis properties

Three samples run on the MiniMag VSM revealed coercive forces ( $H_c$ ) and RACF values ranging between 10 and 40 mT and 36 and 80 mT, respectively, in general accordance with the IRM acquisition experiments. Values of the ratio  $M_c/M_{rs}$  range between 0.08 and 0.35, indicative of magnetite in pseudo- to single-domain states (PSD/SD) (Dunlop 1981). The rock-magnetic properties of sediments from the different caves and stratigraphic levels are rather uniform, suggesting small variations in source material.

### Anisotropy of magnetic susceptibility (AMS)

The magnetic fabric is specified by the directions and lengths of the maximum, intermediate and minimum principal axes

( $k_1, k_2, k_3$ ) of the susceptibility ellipsoid determined from 15 measurements of susceptibility along different axes. Magnetic fabric results are summarized in Figs 9, 11 and 12. The fabric is described by the ratios  $P1 = k_1/k_2$  (lineation),  $P2 = k_1/k_3$  (anisotropy),  $P3 = k_2/k_3$  (foliation) and  $E = k_2^2/k_1 k_3$  (ellipticity) (Ellwood, Hroudin & Wagner 1988). The directional as well as scalar parameters of AMS again reveal rather uniform properties in these sediments.

A well-developed magnetic fabric is present in all samples ( $N = 145$ ) with anisotropies ( $P2$ ) ranging from 1.043 to 1.343 (mean:  $1.019 \pm 0.012$ ) and completely dominated by foliation ( $P3$ ) (oblate ellipsoids  $E > 1$ ) which ranges from 1.025 to 1.316 (mean:  $1.175 \pm 0.067$ ) indicative of a predominantly gravity-controlled grain alignment. The  $k_1$ -axes define subhorizontal foliation planes, dipping between  $1^\circ$  and  $20^\circ$  in general accordance with the visual lamina structures.

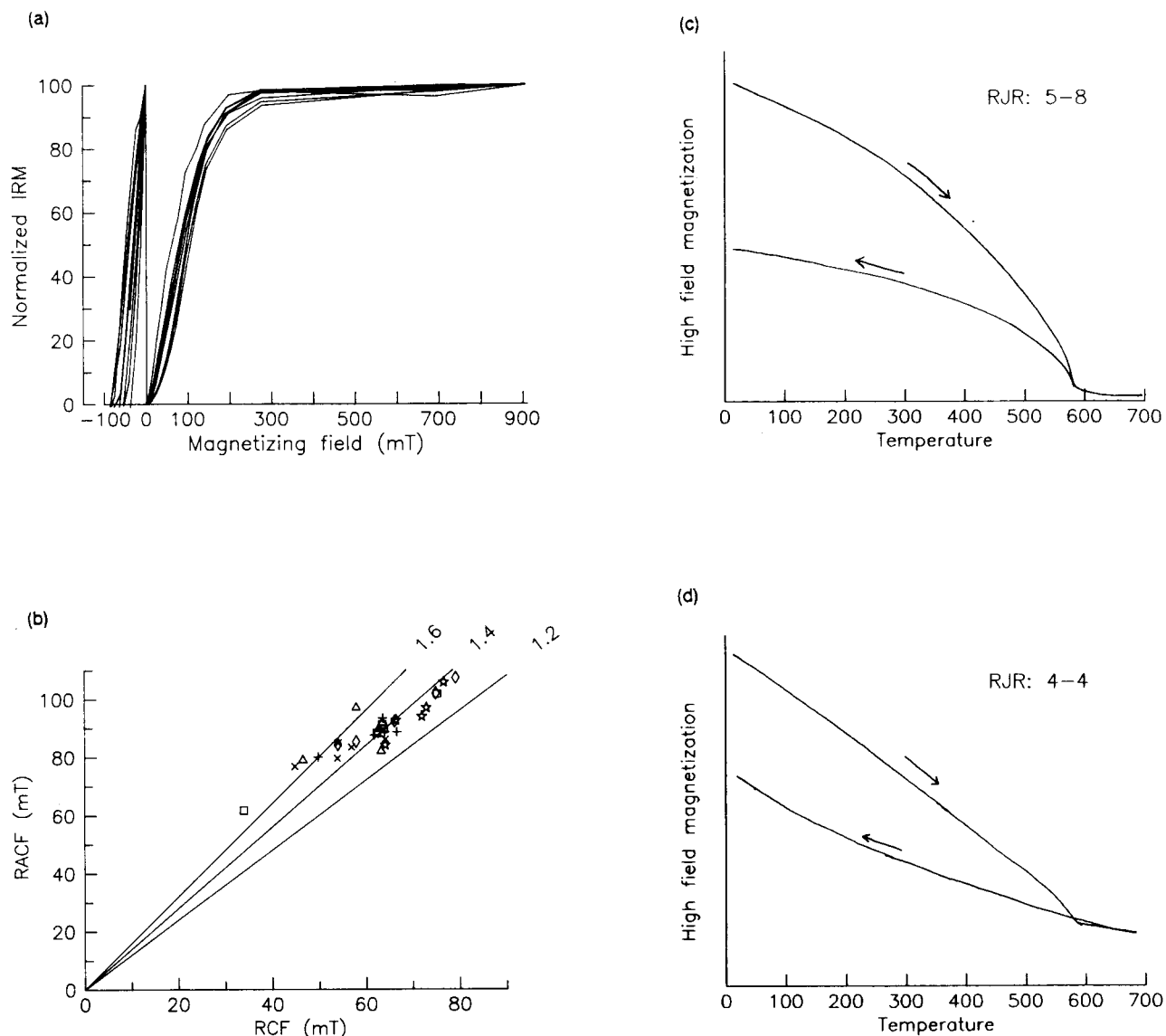


**Figure 8.** (a) Acquisition curves of isothermal remanent magnetization (IRM) of representative samples from all sites exhibit comparable features indicating uniform compositions of magnetic minerals. (b) Remanent acquisition coercive force (RACF) versus remanent coercive force (RCF) for samples in this study. Straight lines drawn for RACF/RCF-ratios of 1.2, 1.4 and 1.6. Samples from different U-channels are depicted by different symbols: 1 (square), 2 (triangle), 3 (diamond), 4 (star), 5 (plus) and 6 (cross). The confined distribution does not reveal any systematic differences between the sites. (c) and (d) Thermomagnetic curves exhibiting typical features of the cave sediments from the Hellemofjord area. Heating/cooling curves indicated by arrows. Temperature scale in °C. High field magnetization axis, arbitrary units.

## PROPERTIES OF NRM

The intensities of natural remanent magnetization (NRM) in the different sediment sections range between 10 and  $800 \text{ mA m}^{-1}$ , while susceptibilities have a comparable range varying between 2 and  $80 \times 10^{-4} \text{ SI}$ .

### A.f. demagnetization

Progressive a.f. demagnetization at an applied field of 5 mT removed in some samples a small magnetic component deviating slightly ( $<10^\circ$  of arc) from the single-component magnetization isolated at higher a.f. fields (Fig. 12). Above

5–10 mT and up to the highest applied demagnetization field (70 mT), all samples carry a single palaeomagnetic component defined by a linear segment approaching the origin of the orthogonal vector plots (Fig. 12). Median destructive field (MDF) values range between 20 and 60 mT, and are related to the lithology, in that visually coarser sediments (sands–silts) have lower MDFs (16–38 mT) compared with the almost pure clay samples (MDF: 45–70 mT). The overall mean of  $50.3 \pm 20 \text{ mT}$  is consistent with the presence of fine-grained magnetite, in accordance with the rock-magnetic properties.

Characteristic remanent directions (ChRM) were calculated by the IAPD line find program (Torsvik 1992), which resulted in a data set indistinguishable from corresponding directions defined by a.f. demagnetization to 20 mT.



**Directional properties**

*Rågge Javre Raigi: Site 1*

Stratigraphic variations of palaeomagnetic directions and bulk properties in this small sediment-filled depression are, in general, associated with visible lithological boundaries (Fig. 4). A single, laminated silt-clay layer (Ca and Cb, Fig. 4) is the only correlatable stratigraphic unit between the limb and central part of the 'basin'. This unit carries a smooth record of declination turning from the east towards due north, associated with inclinations which are too shallow to represent a Quaternary geomagnetic field at this latitude. Units Da, Ea and Fa consist of clay clasts embedded in a silty matrix showing microtectonic shear planes; the remaining units appear visually undeformed.

*Site 2*

Palaeomagnetic directions from the clay-silt layers in the three pits comprising Site 2 reveal rather tight directional distributions which show significant deviations, however, between the pits (Fig. 9). This may reflect influence of water

flow during deposition or slight deformation caused by human foot pressure. Alternatively, the samples from the three pits might not represent a synchronous unit, implying that the deviations may represent genuine records of geomagnetic field variations preserved in laterally accreted sediments.

*Site 3*

The most extensive section from this pit was sampled by two U-channels overlapping by some 10 cm. The overlapping sections reveal quite similar variations, as seen in the composite stratigraphic plot of Fig. 7. Units C, D and E are also present in the single U-channel collected close to the corner of the passage where they exhibit comparable variations in magnetic properties.

*Noroldakh-Raigi and Østhullet*

The directional distributions from the three sites in these caves are rather steep-dipping and fairly well grouped (Fig. 10).

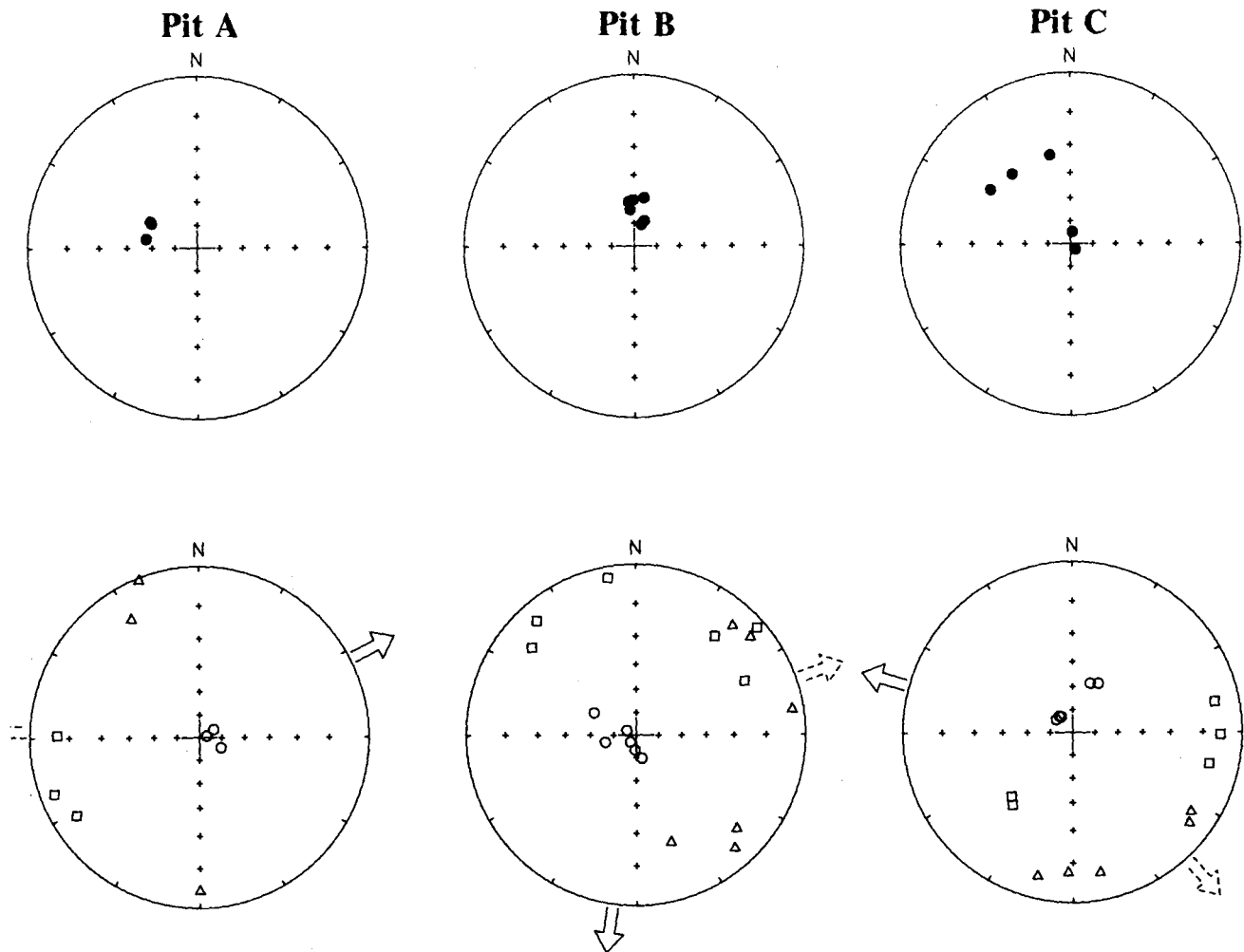


**Fig. 9.** Rågge Javre Raigi cave Site 2: stereographic projection showing distributions of ChRM (top) and principal susceptibility axes ( $m$ ) from the three pits A, B and C. All points are plotted in the lower hemisphere. ChRM, filled circles. Principal susceptibility axes, symbols:  $k_1$ , square;  $k_2$ , triangle;  $k_3$ , circle. Solid arrow, calculated average flow direction; broken arrow, dip direction of magnetic on planes.

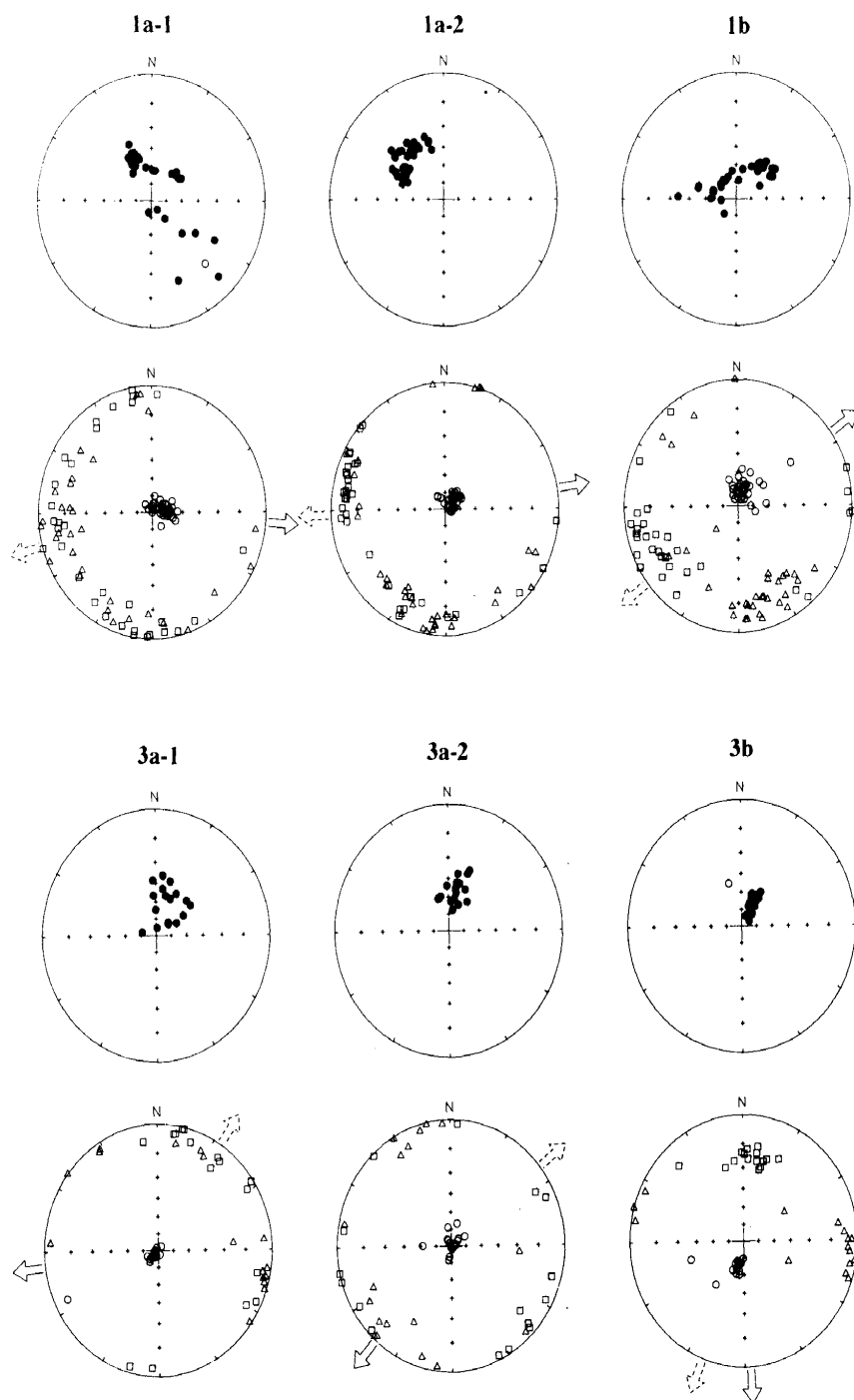


**Figure 11.** Stereographic projections of ChRM (filled symbols) and principal susceptibility axes (open symbols) from Site 1 (reference section, 1a-1 and 1a-2; eastern part, 1b) and Site 3 (3a-1 and 3a-2, central part; 3b, close to the corner/wall). Solid arrow, calculated flow direction; broken arrow, dip direction of magnetic foliation planes.

sections from Sites 1 and 3 may be partly attributed to such effects.

**Inclination error**

Redeposition experiments of sand-silt-sized sediments have demonstrated that the inclinations of DRM are systematically shallower than the ambient field inclination (King 1955). The relationship between inclinations of the DRM ( $I_{\text{DRM}}$ ) and of the external magnetic field ( $I_{\text{Hex}}$ ) is described by the empirical expression  $\tan(I_{\text{DRM}}) = 0.4 \tan(I_{\text{Hex}})$  (King 1955). This relationship implies that at 67°N the inclination error would cause a DRM to carry an inclination of the order of 60°, compared with the axial geomagnetic field inclination of 77°. There are presently no methods for correcting inclination errors in general. A quantitative model for correcting inclination errors, based on the

anisotropy of magnetic susceptibility (AMS) or anhysteretic remanent magnetization (ARM) has recently been proposed (Jackson *et al.* 1991). However, the model requires that magnetic moments are parallel to the long axis of grains (maximum susceptibility/ARM), an assumption which is challenged by recent experiments on pDRM properties of PSD magnetite grains (Løvlie 1992). Applying the classical correction for inclination error ( $\tan(I_{\text{DRM}}) = 0.4 \tan(I_{\text{Hex}})$ ) to the results obtained in this study yields directional distributions with inclinations in general accordance with the Quaternary geomagnetic field, suggesting that the sediments carry an initial DRM affected by inclination error.

**PALAEOMAGNETIC STRATIGRAPHY**

The similarities in depositional environment and lithological properties may justify correcting ChRM directions for the

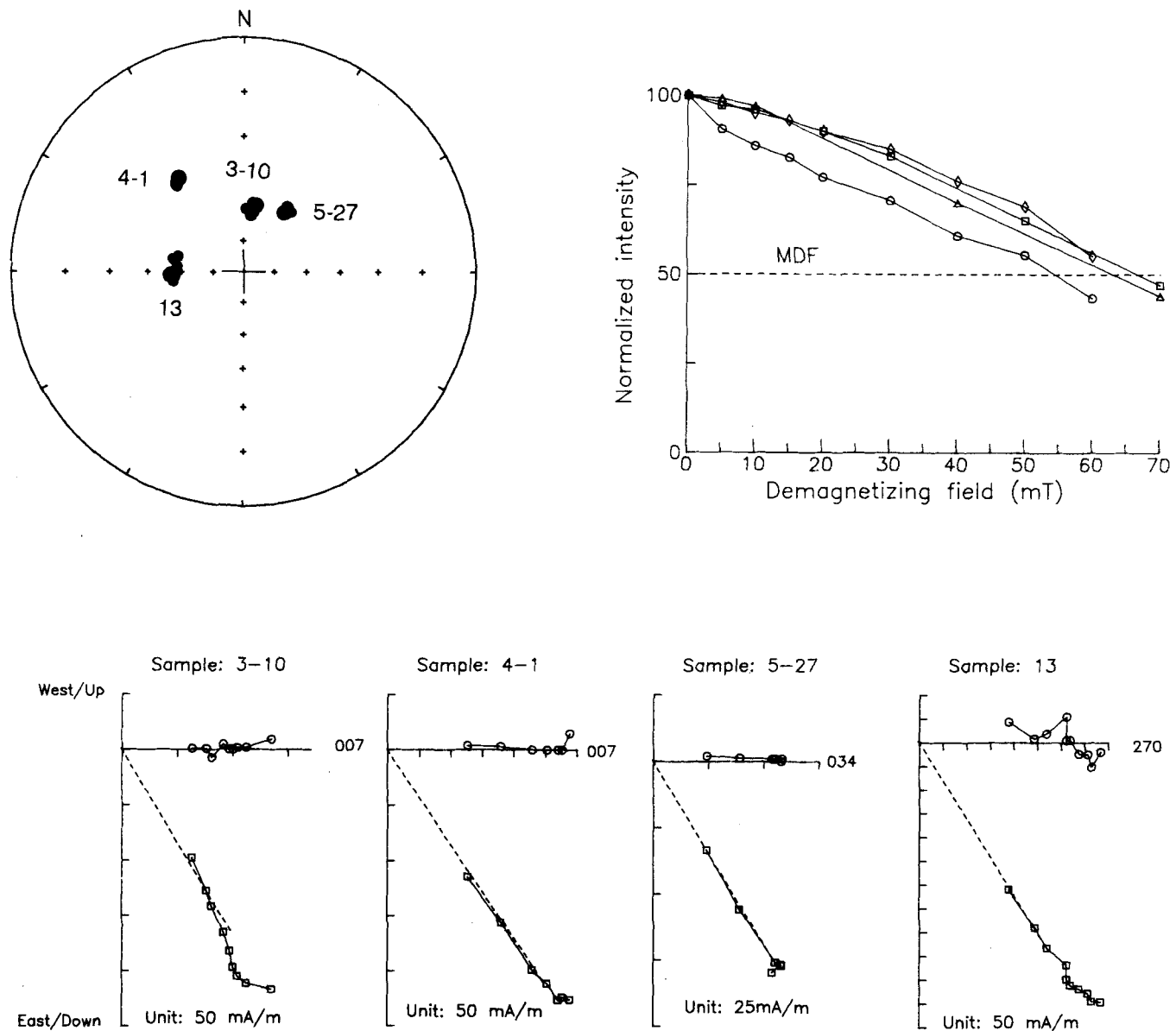


**Figure 12.** Examples of a.f.-demagnetization behaviour of cave sediment samples shown on stereographic and optimal orthogonal projections together with normalized intensity curves for samples from Site 1 (3-10, 4-1, 5-27) and Site 2 (13). The characteristic component is indicated by a broken line on the orthogonal plots. MDF is the intensity level for determination of the median destructive field.

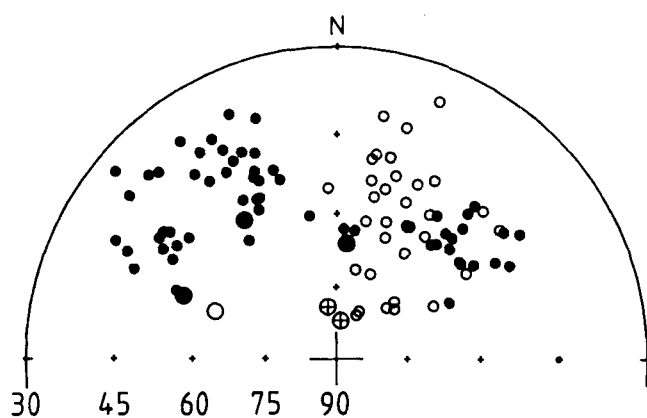


**Figure 13.** Stereographic distribution of ChRM directions for all samples and sites. Note the expanded stereographic projection showing inclinations between 30° and 90°. Symbols: small filled circles, Site 1 (560 m a.s.l.); large filled circles, mean directions Site 2 (550 m a.s.l.); small open circles, Site 3 (120 m a.s.l.); large open circles, mean directions Østhullet; circles with cross, Noroldakhraigi (670 m a.s.l.). Note: all symbols depict lower hemisphere.

probable inclination error. However, stratigraphic correlations may, for the same reason, be based on the observed and uncorrected ChRM directions.

The palaeomagnetic directions represent records of geomagnetic field variations of different time-spans retained in sediments at different heights above sea-level. In stereographic projection, ChRM directions from the different sites define almost a closed loop, confined between 70°E and 70°W with inclinations from 32° to 85° (Figs 11 and 13). A clockwise rotation of the palaeomagnetic vectors can be inferred from the systematic eastward change in directions from the two investigated stratigraphic sequences at Site 1. Coinciding directional distributions are apparent for declinations and inclinations around 330° and 50°, respectively (Fig. 13). The top unit at Site 1 correlates fairly well with the distribution of directions from the Site 3 section, implying that deposition in the lower part of the cave (120 m) occurred after the small deposit at 560 m had accumulated.

The 'spot' readings of the samples from the three pits constituting Site 2 also match the general directional path defined by the record from Site 1.

The significantly more steeply dipping directions from the Noroldakh-Raigi and Østhullet sites apparently define the closing of a near-sided, clockwise-rotating directional loop. The chronological relationships are in reasonable agreement with the altitudes of the different sites, suggesting that sediment accumulation occurred at the highest localities first. On the assumption that the sites describing the almost closed palaeomagnetic loop probably represent incomplete records of succeeding depositional events during one subglacial event, the results are consistent with an inverse depositional stratigraphy.

## DISCUSSION AND CONCLUSION

The anomalously low palaeomagnetic inclinations in the investigated unconsolidated cave sediments are attributed to

the inherent property of DRM to acquire shallow remanent directions. More or less physically realistic models have been proposed for the acquisition of DRM (King 1955; Griffiths *et al.* 1960) and pDRM (Otofujii & Sasajina 1981), but none possess any predictive potential. Consequently there is no general method to distinguish between a DRM and pDRM. Considering that lacustrine and marine sediments of comparable grain sizes to the present cave sediments apparently record geomagnetic field variations with a high fidelity, inclination error is probably not a common feature in nature. It is proposed that this may be due to the action of different post-depositional, environmentally dependent processes causing post-depositional realignment of magnetic grains (Clegg, Almond & Stubbs 1954; Løvlie 1989b). This suggestion is partly based on the observation that inclinations of DRM in slowly deposited, disintegrated natural or synthetic sediments produced in the laboratory may be shallower than the ambient magnetic field as opposed to directions of remanent magnetization acquired after stirring the same sediment (Tucker 1980). In contrast to lacustrine, fluvial and marine sediments, the biologically sterile deep cave sediments are not exposed to post-depositional processes affecting the spatial arrangement of mineral grains (e.g. burrowing). Deep cave environments maintain an almost constant temperature equivalent to the mean annual temperature outside the cave, as opposed to 'subaerial' sediment accumulation in rivers and lakes which may be exposed to small, but daily, and certainly seasonal, temperature variations. It is proposed that these small temperature variations in addition to biological (bioturbation) and chemical (precipitation of gels) processes effectively may cause the acquisition of pDRM explaining the high palaeomagnetic fidelity of most fine-grained sediments. PDRM has recently also been demonstrated to occur in shallow marine (fjord) sediments exposed to the weak diurnal tides as well as wave action (Løvlie 1989b). It is hence concluded that the present cave sediments have retained the initial DRM acquired at the time of deposition, justifying corrections of the inferred inclination error.

## Duration and chronostratigraphy

The anomalously low inclinations, which are compatible neither with Weichselian nor Holocene lacustrine PSV records (Creer & Tucholka 1982; Sandgren 1986; Thouveny, Creer & Blunk 1990) corrected for latitude by the conversion via pole (CVP) procedure (Noel & Batt 1990), have been corrected for the inclination error by applying the previously presented trigonometric expression. The major directional pattern is maintained after correction, but inclinations are now in general agreement with a Late Weichselian geomagnetic field configuration (Fig. 14).

On the assumption that the Hellemofjord records represent discrete, but succeeding, time-readings of geomagnetic field variations, the amplitude in declination of the inferred almost closed loop suggests a minimum duration of some 400 years when compared with historical observatory records since 1600. A more realistic approach, comparison with pre-Holocene PSV records, is not possible due to the lack of high-precision Late Weichselian PSV records from the latitudes in question. Correlations must hence rely on

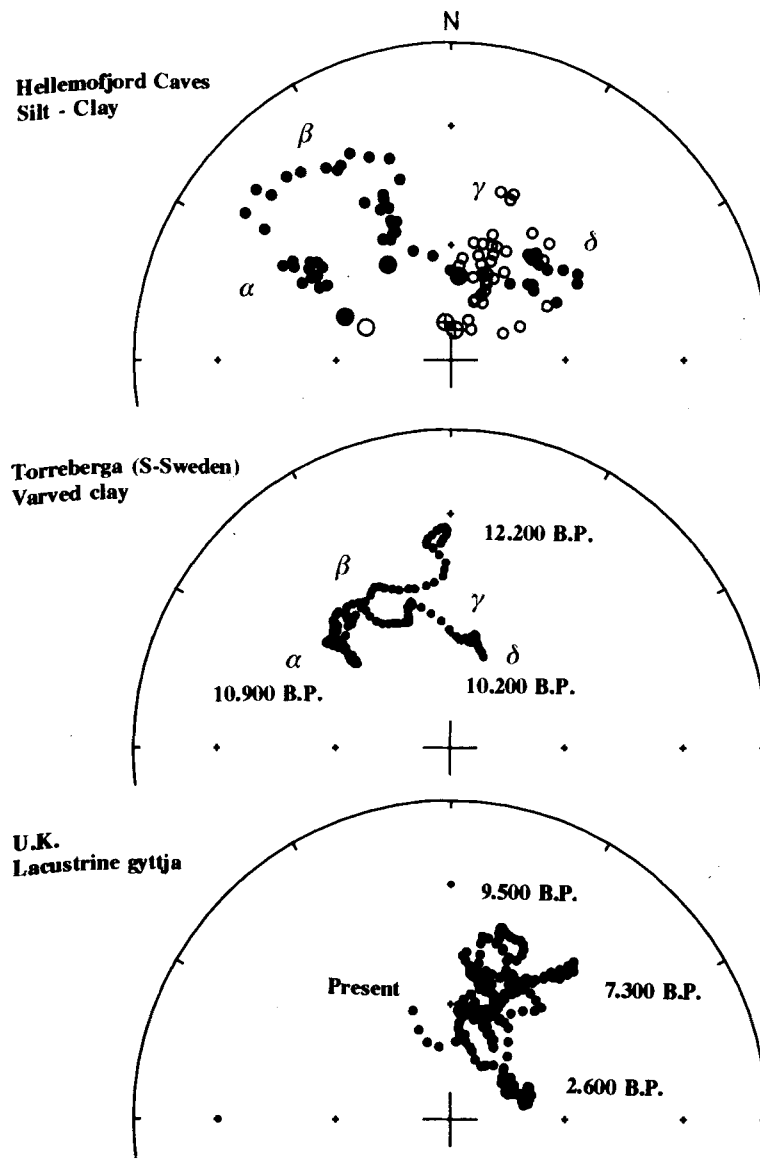


**Figure 14.** Expanded stereographic projections of the Hellemofjord cave sediment palaeomagnetic directions (three-point univectorial running mean) after correcting for the classical inclination error (top); five-point univectorial running mean of the Torreberga varved clays converted via pole to site location (15°E and 67°N) (middle diagram); and five-point univectorial running mean of the UK master curve for the Holocene also converted via pole to site location. Correlating features (Hellemofjord–Torreberga) indicated by  $\alpha$ ,  $\beta$ ,  $\gamma$  and  $\delta$ . All symbols lower hemisphere. For legend of top diagram, see Fig. 13.

CVP corrected records from sites 10°–15° of latitude further to the south. The CVP procedure apparently introduces errors of the order of less than 2° in declination and inclination when applied to sites some 2000 km apart (Noel & Batt 1990). Applying the CVP procedure on the International Geomagnetic Reference Field between 15°W and 30°E and 50°N and 74°N we have found comparable deviations in declination and inclination. CVP corrections to the locality in question (67°N/15°E) have been performed on the UK Holocene master curve (Thompson & Turner 1979) as well as the pre-Holocene PSV record retained in varved clays sequences from Torreberga, Southern Sweden (Sandgren 1986) (Fig. 14).

The declination range of the Hellemofjord record appears to fall within the combined ranges of the Torreberga

(12 000–10 200 BP) and UK master curves (10 000–Present) confined in the westerly (pre-Holocene) and easterly (Holocene) quadrants, respectively (Fig. 13). The UK palaeosecular variation curves exhibit several directional crossing points, illustrating the inherent ambiguity associated with the independent application of high-resolution PSV records for chronostratigraphic correlations.

On the assumption that the Hellemofjord sediments accumulated during the final Late Weichselian glacial retreat, and allowing for directional deformations introduced by the CVP procedure, the inclination-corrected Hellemofjord curve exhibits some distinct directional features also recognized on the Torreberga curve,  $\alpha$ – $\beta$ – $\gamma$  (Fig. 14). Adopting this correlation, the Rågge Javre Raigi sediments at 560 m altitude hence accumulated between c. 10 900 and

10 200 BP. The eastward, scattered distribution ( $\delta$  Fig. 14), represents the lowermost sediments in Rågge Javre Raigi, exhibiting no systematic stratigraphic pattern and falling within the Holocene directions derived from the UK curve. The absence of systematic stratigraphic variations prevents further chronostratigraphic considerations.

This exercise tentatively suggests a duration of sediment accumulation in Rågge Javre Raigi of the order of 700 years, commencing around 10 900 BP.

The inferred geomagnetic spot readings retained in the Noroldahk Raigi and Østhullet sediments are not readily correlated with either of the reference curves. This may indicate that these sections do not record genuine geomagnetic field directions, or alternatively, that they accumulated within time windows prior to 12 200 BP.

## ACKNOWLEDGMENTS

We acknowledge the conscientious assistance in the field by J. Kyselak, P. Sevcik, J. Sevcikova, R. Blazek, J. Svoboda, T. I. Korneliussen, and in the laboratory by K. Breyholtz and V. Valen. We are also grateful to C. Laj and C. Kissel for the opportunity to run samples on the VSM in the Gif sur Yvette laboratory. Constructive comments from E. Hailwood and two anonymous referees greatly improved the clarity of this paper. P. Sandgren kindly supplied the Torreberga data record. This is a contribution to the 'KLIMBRE'-project funded by the Norwegian Research Council for Science and the Humanities.

## REFERENCES

- Blow, R.A. & Hamilton, N., 1978. Effect of compaction on the acquisition of a detrital remanent magnetization in fine-grained sediments, *Geophys. J. R. astr. Soc.*, **52**, 13–23.
- Cande, S.C. & Kent, D.V., 1992. A new geomagnetic polarity time scale for the Late Cretaceous and Cenozoic, *J. geophys. Res.*, **97**, 13 917–13 951.
- Cisowski, S., 1981. Interaction vs. non-interaction single domain behaviour in natural and synthetic samples, *Phys. Earth planet. Inter.*, **26**, 56–62.
- Clegg, J.A., Almond, M. & Stubbs, P.H.S., 1954. The remanent magnetism of some sedimentary rocks in Britain, *Phil. Mag.*, **45**, 583–598.
- Creer, K.M. & Kopper, J.S., 1974. Paleomagnetic dating of cave paintings in Tito Bustillo cave, Asturias, Spain, *Science*, **186**, 348–350.
- Creer, K.M. & Kopper, J.S., 1976. Secular oscillations of the geomagnetic field recorded by sediments deposited in caves in the Mediterranean region, *Geophys. J. R. astr. Soc.*, **45**, 35–58.
- Creer, K.M. & Tcholka, P., 1982. Secular variation as recorded in lake sediments: a discussion of North American and European results, *Phil. Trans. R. Soc. Lond.*, A, **306**, 87–102.
- Dankers, P., 1981. Relationship between median destructive field and remanent coercive force for dispersed natural magnetite, titanomagnetite and hematite, *Geophys. J. R. astr. Soc.*, **64**, 447–461.
- Dunlop, D.J., 1981. The rock magnetism of fine particles, *Phys. Earth planet. Inter.*, **26**, 1–26.
- Ellwood, B.B., Hrouda, F. & Wagner, J.J., 1988. Symposia on magnetic fabric: introductory comments, *Phys. Earth planet. Inter.*, **51**, 249–252.
- Gravenor, C.P., Symons, D.T.A. & Coyle, D.A., 1984. Errors in the anisotropy of magnetic susceptibility and magnetic remanence of unconsolidated sediments produced by sampling methods, *Geophys. Res. Lett.*, **1**, 836–839.
- Griffiths, D.H., King, R.F., Rees, A.I. & Wright, A.E., 1960. The remanent magnetism of some recent varved sediments, *Proc. R. Soc. Lond.*, A, **256**, 359–383.
- Hailwood, E., Stumpp, C. & Zudin, J., 1989. Soft sediment sampling errors in palaeomagnetic fabric data, *IAGA Bull. No.* 53, 199.
- Hamilton, N., 1967. The effect of magnetic and hydrodynamic control on the susceptibility anisotropy of redeposited silt, *J. Geol.*, **75**, 738–743.
- Hamilton, N. & King, R.F., 1964. Comparison of the bedding errors of artificially and naturally deposited sediments with those predicted from a simple model, *Geophys. J. R. astr. Soc.*, **8**, 370–374.
- Jackson, M.J., Banerjee, S.K., Marvin, J.A., Lu, R. & Gruber, W., 1991. Detrital remanence, inclination errors and anhysteretic remanence anisotropy: quantitative model and experimental results, *Geophys. J. Int.*, **104**, 95–103.
- King, R.F., 1955. The remanent magnetism of artificially deposited sediments, *Mon. Not. R. astr. Soc.*, **7**, 115–134.
- Kodama, K.P. & Sun, W.W., 1992. Magnetic anisotropy as a correction for compaction-caused palaeomagnetic inclination shallowing, *Geophys. J. Int.*, **111**, 465–469.
- Lauritzen, S.E., Kyselak, J. & Løvlie, R., 1991. A new survey of Råggejavri-Raigi and the Hellemofjord Karst, Norway, *Cave Sci.*, **18**, 131–137.
- Løvlie, R., 1989a. Magnetic stratigraphy: a correlation method, *Quat. Int.*, **1**, 129–149.
- Løvlie, R., 1989b. Magnetization of sediments and depositional environment, in *Geomagnetism and Palaeomagnetism*, pp. 243–252, eds Lowes, F.J., Noel, M., Ruduicki, M.D., Kluwer Academic Publishers.
- Løvlie, R., 1992. Experimental determination of the relationship between magnetic moment and grain geometry of natural magnetite, *Phys. Earth Planet Inter.*, **76**, 105–112.
- Løvlie, R., Gilje-Nilsen, H. & Lauritzen, S.E., 1988. Revised magnetostratigraphic age estimate of cave sediments from Grønligrotta, Norway, *Cave Sci.*, **15**, 105–108.
- Løvlie, R., Markussen, B., Sejrup, H.P. & Thiede, J., 1986. Magnetostratigraphy in three Arctic Ocean sediment cores; arguments for geomagnetic excursions within oxygen-isotope stage 2–3, *Phys. Earth planet. Inter.*, **43**, 173–184.
- Noel, M., 1986. An anomalous detrital sediment magnetization, *Geophys. J. R. astr. Soc.*, **78**, 231–239.
- Noel, M., 1987. The magnetostratigraphy of cave sediments in Masson Hill, Derbyshire, *Proc. York. Geol. Soc.*, **46**, 193–201.
- Noel, M. & Ruduicki, M.D., 1988. A computer program for determining current directions from rock magnetic data, *Comput. Geosci.*, **14**, 321–338.
- Noel, M. & St. Pierre, S., 1984. The paleomagnetism and magnetic fabric of cave sediments from Grønligrotta and Jordbruks-grotta, Norway, *Geophys. J. R. astr. Soc.*, **78**, 231–239.
- Noel, M. & Batt, C.M., 1990. A method for correcting geographically separated remanence directions for the purpose of archeomagnetic dating, *Geophys. J. Int.*, **102**, 753–756.
- Rees, A.I., 1961. The effect of water currents on the magnetic remanence and anisotropy of susceptibility of some sediments, *Geophys. J. R. astr. Soc.*, **5**, 235–251.
- Rees, A.I., 1966. The effect of depositional slopes on the anisotropy of magnetic susceptibility of laboratory deposited sands. *J. Geol.*, **74**, 856–867.
- Sandgren, P., 1986. Late Weichselian palaeomagnetic secular variation from the Torreberga basin, South Sweden, *Phys. Earth planet. Inter.*, **43**, 160–172.

- Thompson, R., 1983. <sup>14</sup>C dating and magnetostratigraphy, *Radiocarbon*, **25**, 229–238.
- Thompson, R. & Turner, G.M., 1979. British geomagnetic master curve 1,000–0 yr. B.P. for dating European sediments, *Geophys. Res. Lett.*, **6**, 249–252.
- Thouveny, N., Creer, K.M. & Blunk, I., 1990. Extension of the Lac du Bouchet palaeomagnetic record over the last 120,000 years, *Earth planet. Sci. Lett.*, **97**, 140–161.
- Torsvik, T.H., 1992. *IAPD—Interactive Analysis of Paleomagnetic Data* (program manual), Norwegian Geological Survey, Trondheim.
- Tucker, P., 1980. Stirred remanent magnetization: A laboratory analogue of post-depositional realignment, *J. Geophys.*, **48**, 153–157.
- Verosub, K.L., 1977. Depositional and post-depositional processes in the magnetization of sediments, *Rev. Geophys. Space Phys.*, **15**, 129–143.